University of Sistan and Baluchestan

Chemical Process Design

Available online at http://cpd.usb.ac.ir/

Vacuum Drying of Magnesium Hydroxide using Steelmaking Ladle Hot Air as an Alternative Heat Source

Afsaneh Sadeghi Goghari[1], Hossein Maghsoudi[2]✉, Ahmad Ghazanfari Moghaddam[3], Kazem Jafarinaeimi[4]

[1] Biosystems Engineering Department, Shahid Bahonar University of Kerman, Kerman, Iran. Email: afsaneh.sadeghi@eng.uk.ac.ir
[2] Corresponding Author, Biosystems Engineering Department, Shahid Bahonar University of Kerman, Kerman, Iran. Email: h.maghsoudi@uk.ac.ir
[3] Biosystems Engineering Department, Shahid Bahonar University of Kerman, Kerman, Iran. Email: aghazanfari@uk.ac.ir
[4] Biosystems Engineering Department, Shahid Bahonar University of Kerman, Kerman, Iran. Email: jafarinaeimi@uk.ac.ir

ARTICLE INFO

Article type:
Research Article

Article history:
Received: 2026-03-12
Received in revised form: 2026-04-13
Accepted: 2026-04-19
Available online: 2026-04-19

Keywords: *Drying; Desalination Brine; Statistical analysis; Mathematical modeling*

ABSTRACT

The growing application of magnesium in strategic industries underscores the need for sustainable and energy-efficient routes for producing high-purity magnesium compounds. In this study, a vacuum drying system was designed and fabricated to enable the recovery of magnesium hydroxide from desalination effluent, and its drying performance was evaluated. Experiments were carried out at three operating pressures (0.10, 0.05, and 0.02bar) and three temperatures (150, 210, and 250°C), utilizing hot air recovered from steelmaking ladles as an industrial waste-heat source. The results showed that reducing the operating pressure significantly decreased the drying time while enhancing the mass transfer rate. At 0.02 bar, the time required to reach the target final moisture content was markedly shorter than that at 0.10 bar, with an average reduction of approximately 50%. Moreover, increasing the drying temperature from 150 to 250°C led to a substantial acceleration of the drying process, resulting in an overall reduction of 69.2% in total drying time. Drying kinetics were analyzed using logarithmic and two-term exponential models. Statistical evaluation revealed that the logarithmic model provided superior predictive performance, exhibiting a high coefficient of determination (R^2 =0.99) and lowest root mean square error (RMSE=0.012) across all operating conditions. Overall, this study demonstrates that the integration of vacuum drying with the utilization of steelmaking waste heat represents an efficient and sustainable approach for the recovery of magnesium hydroxide from desalination effluents, offering both technical effectiveness and industrial relevance.

Cite this article: Sadeghi Goghari, A., Maghsoudi, H., Ghazanfari Moghaddam, A., Jafarinaeimi, K., (2026), Vacuum Drying of Magnesium Hydroxide using Steelmaking Ladle Hot Air as an Alternative Heat Source, *Chemical Process Design*, 5(2), 00-00. http//doi.org/10.22111/cpd.2026.54993.1086

DOI: http//doi.org/10.22111/cpd.2026.54993.1086

Publisher: University of Sistan and Baluchestan.

1. Introduction

Magnesium (Mg) is widely recognized as a strategic material in modern industry. It is the lightest structural metal used in engineering applications. Magnesium and its compounds are used in automotive, aerospace, transportation, and electronics industries due to their low density, high strength-to-weight ratio, and favorable recyclability [1]. Magnesium occurs in seawater at relatively high concentrations, mainly in dissolved ionic forms, and can be converted into magnesium hydroxide, and can be recovered through processes such as electrolytic methods, ion-exchange resins, adsorption, and membrane-based techniques [2].

From an environmental perspective, magnesium is important in industrial and marine effluent management. Large volumes of wastewater are generated by desalination, steelmaking, and petrochemical industries, often enriched with Mg^{2+} ions. Improper increases salinity and environmental stress in aquatic systems [3]. Consequently, recovering magnesium from industrial effluents and converting it into magnesium hydroxide, is aligned with circular economy principles. For instance, desalination brine contains approximately 1717mg/L of magnesium ions. With a daily brine flow of about 46,080m^3, this corresponds to roughly 79 tons of magnesium per day, (≈0.17wt%).

Various methods are used for magnesium hydroxide recovery from brines and wastewater. Their efficiency depends on Mg^{2+} concentration, solution chemistry, and energy demand. Chemical precipitation is widely used, but it requires high reagent consumption for dilute streams. Therefore, pre-concentration via water removal is essential to improve process efficiency and reduce chemical usage. This makes energy-efficient processing of magnesium hydroxide from secondary resources—especially industrial effluents and desalination brines—highly important.

Water evaporation combined with magnesium hydroxide precipitation is a conventional method in magnesium processing. Evaporation directly controls supersaturation, precipitation behavior, and overall energy consumption. This method can be implemented using solar or industrial heating systems, including vacuum-assisted evaporation. Compared with advanced separation technologies such as membrane processes and ion-exchange systems (Fig. 1), which are typically associated with higher capital and operating costs, evaporation as a pre-concentration step offers a simple, effective, and sustainability-oriented solution for magnesium recovery.

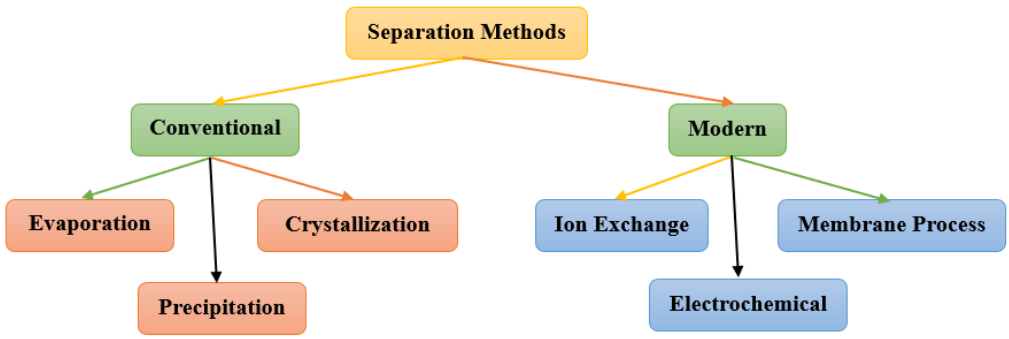

Fig. 1. Classification of conventional and modern separation methods chemical industries

Drying and evaporation processes rely on coupled heat and mass transfer mechanisms. Moisture moves internally toward the surface and is then removed to the surrounding environment. These interactions strongly influence drying kinetics [4]. Vacuum dryers are particularly suitable for heat- sensitive materials because they operate under reduced pressure and low-oxygen conditions [5]. Lower pressure reduces the boiling point of water, enabling evaporation at lower temperatures and minimizing thermal degradation. Recent studies show that vacuum drying improves product quality compared with conventional methods [6].

Vacuum drying also reduces oxidation by limiting oxygen availability, which improves product purity, and prevents discoloration [7]. It is widely used in pharmaceutical, food, and mineral processing industries [8]. However, despite extensive studies on vacuum drying, limited attention has been given to integrating vacuum drying systems with industrial waste-heat recovery.

In the present study, magnesium hydroxide ($Mg(OH)_2$) was recovered from the effluent of the desalination unit at Hormozgan Steel Company through chemical precipitation using a sodium hydroxide (NaOH) solution. After precipitate formation and filtration, the samples were dried in a custom-designed vacuum dryer to remove free moisture and enhance final product purity. The primary objective of this work was to investigate the effects of operating temperature and pressure on drying time and to model the associated drying kinetics of magnesium hydroxide recovery from desalination effluent. This study addresses a key research gap by integrating vacuum drying with industrial waste heat from steelmaking ladles for magnesium hydroxide valorization, a topic that has received limited quantitative and experimental investigation. Unlike conventional studies focused solely on controlled energy input, this work utilizes real industrial waste heat under low-pressure conditions to achieve a more sustainable drying process. The novelty of this study lies in the combined experimental implementation of this system and the quantitative evaluation of its drying performance under varying temperature and vacuum conditions, providing new insights into the coupling of resource recovery and energy reutilization in mineral processing.

2. Materials and methods

2.1. Effluent sampling and characterization

The experiments for magnesium hydroxide recovery from desalination effluent were conducted at the desalination unit of Hormozgan Steel Company during the summer of 2025. To determine the elemental and chemical composition of the effluent, samples were transferred to the company's laboratory and initially allowed to stand at ambient temperature for 24h to enable gravitational settling of coarse suspended solids. The supernatant liquid was subsequently passed through a stainless-steel filter with a mesh size of 400 (38μm) to remove residual suspended particles and to obtain a homogeneous liquid phase for further analyses.

The filtered effluent was subjected to chemical precipitation using a sodium hydroxide (NaOH) solution, followed by solid–liquid separation. The chemical precipitation was performed under controlled conditions. The initial concentration of Mg^{2+} in the effluent was determined to be 0.0706mol/L. Precipitation was carried out using NaOH based on the stoichiometric reaction (Eq. (1)):

$$Mg^{2+} + 2NaOH \rightarrow Mg(OH)_2 \downarrow \quad (1)$$

This reaction requires a molar ratio of 2:1 ($NaOH:Mg^{2+}$). Therefore, the stoichiometric amount of NaOH needed was calculated as 0.1412mol/L, equivalent to 5.65 g/L. To ensure complete reaction and achieve optimal removal efficiency, the practical NaOH concentration was adjusted and maintained within the range of 5.6 to 6.0g/L throughout the process [9]. Specifically, an initial NaOH solution (containing 6g in 40mL of distilled water) was added dropwise in several stages to 1 L of pre-heated effluent (heated to 35°C). After 40 minutes of initial addition and mixing, an additional 2g of NaOH was added, and mixing continued for another 10 minutes. During the precipitation process, the pH was monitored and increased from an initial value of 8.3 to approximately 11. This controlled, gradual increase in pH facilitated the formation of stable and larger $Mg(OH)_2$ precipitate particles, which aided in subsequent sedimentation and filtration steps. Under these optimized conditions, the final magnesium

concentration in the solution was reduced to approximately 44mg/L, achieving a magnesium removal efficiency of 97.5%. The elemental composition of both the brine and the $Mg(OH)_2$ precipitates was analyzed using inductively coupled plasma–optical emission spectroscopy (ICP–OES, Varian ES-735). Prior to analysis, solid samples were subjected to alkaline fusion to ensure complete dissolution. The fused samples were subsequently dissolved in diluted nitric acid and filtered before measurement. The ICP–OES analysis was performed under standard operating conditions with axial plasma observation. A flowchart illustrating these process steps and comparing conventional and advanced methods is presented in Fig. 2.

Fig. 2. Overall stages of the desalination brine management process

2.2. Design and fabrication of the vacuum dryer

To perform water evaporation and drying experiments, a laboratory-scale vacuum dryer was designed and fabricated (Fig. 3). The vacuum dryer employed in this study was designed and fabricated adhering to international standards EN and ISO. The main body of the dryer is constructed from EN 1.4539 super duplex stainless steel, chosen for its superior resistance to heat, corrosion, and alkaline environments, making it suitable for contact with magnesium hydroxide precipitate. The inner chamber section was cylindrical in shape and has a height of 40cm, extending to 55cm with the addition of the upper flange. The external diameter of the body is 139.7mm, with a wall thickness of 7.1mm. Connecting pipes are seamless steel conforming to EN 10216-5, with dimensions determined by EN ISO 1127. A rotary vane vacuum pump (model RE 6, VACUUBRAND, Germany) with a maximum pumping capacity of approximately 5.7m^3/h and an ultimate vacuum of 1×10^{-1}mbar (0.01bar) was used, confirming its ability to achieve the required operating pressure.

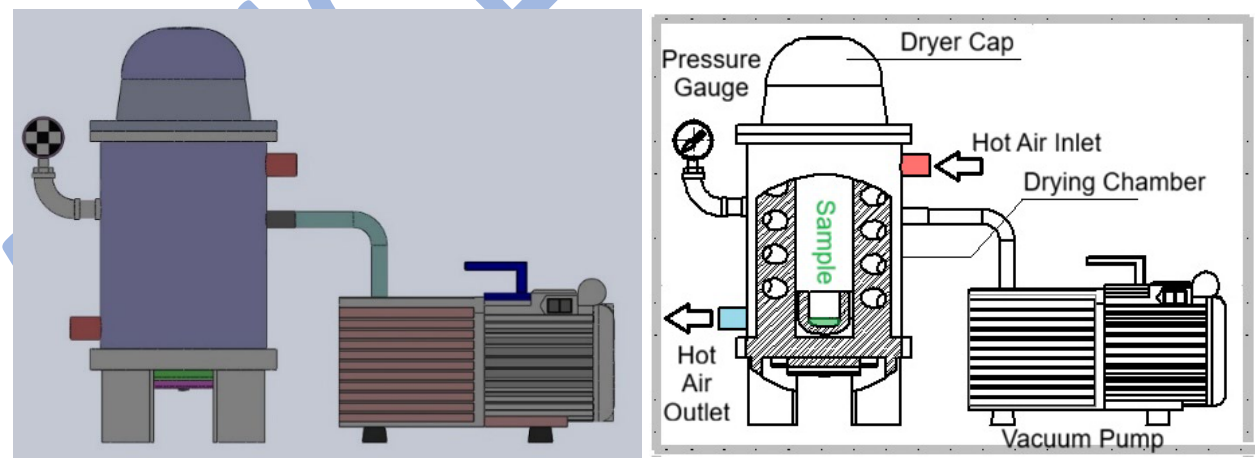

Fig. 3. Three-dimensional view (left) and detailed view (right) of the laboratory-scale vacuum dryer and its major components

For the drying of the magnesium hydroxide precipitate, approximately 100 grams of the wet sediment was placed within the vacuum chamber. The heat source for the drying process was hot air sourced from the vicinity of steelmaking ladles, transferred to the dryer body via heat transfer pipes. This method not only reduced electrical energy consumption but also facilitated the recovery of industrial waste heat [10].

To reduce the boiling point of water during the drying process, the system was equipped with a vacuum unit comprising a mechanical vacuum pump, a vacuum valve, and a pressure gauge, allowing precise control of the internal chamber pressure down to 0.01bar. Pressure reduction not only lowered the boiling point of water but also enhanced the evaporation rate, thereby contributing to the preservation of the quality of the recovered material.

The hot air discharged from a steelmaking ladle (at approximately 600°C and atmospheric pressure) was utilized as the primary heat source for the vacuum dryer, enabling the effective recovery of industrial waste heat. The hot air stream was directed to the dryer body through a steel pipe with a length of 10m and an inner diameter of 6cm, driven by a suction fan with a rated power of 200W. A damper was installed at the inlet of the transfer line to regulate airflow rate and control thermal conditions.

The hot air was introduced into the vacuum dryer through a single inlet pipe connected to the chamber, where the flow was subsequently distributed inside the chamber without a dedicated nozzle or diffuser system. The internal circulation was governed by the inlet momentum and pressure-driven expansion under reduced-pressure conditions, ensuring relatively uniform heat distribution within the drying chamber.

The dryer body temperature was controlled at 150, 210, and 250°C, and the corresponding sample temperatures increased from 20°C to about 60, 68.5, and 75°C, respectively. To minimize heat losses, both the transfer pipes and the dryer body were insulated with rock wool. This insulation significantly improved thermal efficiency, reduced energy losses, and enhanced the operational stability of the system at elevated temperatures.

2.3. Effect of pressure and temperature on drying time

To investigate the combined effects of inlet temperature and vacuum pressure on the drying time, the experiments were designed and conducted based on a randomized complete block design (RCBD) in a full factorial arrangement, involving two factors each at three levels, with three replicates for each treatment combination. The first factor was the dryer wall temperature, set at 150, 210, and 250°C, while the second factor was the absolute pressure inside the drying chamber, adjusted to 0.10, 0.05, and 0.02bar. Drying time was considered as the dependent variable, while temperature and pressure were treated as independent factors.

Accordingly, a total of nine experimental conditions were examined, each performed in duplicate, following a completely randomized factorial design. In each experiment, 100mL of the prepared sample was placed inside the vacuum drying chamber. During drying, the surface temperature of the sample was continuously monitored using a non-contact laser thermometer. Drying time was determined based on the attainment of a stable equilibrium mass under each operating condition. The experimental data were statistically analyzed using analysis of variance (ANOVA) procedures in SPSS software.

2.4. Drying kinetics analysis

The variation in material moisture content during drying is commonly investigated using different mathematical models. To this end, numerous analytical and empirical models have been proposed and applied to describe drying kinetics. In the present study, the drying kinetics of magnesium hydroxide in a vacuum dryer were described using a logarithmic model (Eq. (2)) and a two-term exponential model (Eq. (3)).

$$MR = a * exp(-kt) + c \tag{2}$$

$$MR = a_0 * exp(-k_0 t) + a_1 * exp(-k_1 t) \tag{3}$$

In Eqs. (1) and (2), the moisture ratio (MR) ranges between zero and one, while a, k, c, a_0, a_1, k_0, and k_1 are model constants determined by fitting the models to the experimental data. The logarithmic and two-term exponential models are mathematically capable of describing the nonlinear decreasing behavior of the moisture ratio in drying processes where the drying rate decreases exponentially with time, internal mass transfer resistance is significant, and more than one dominant moisture transfer mechanism—such as the combined effects of internal diffusion and surface evaporation—may occur simultaneously.

The logarithmic model, which is among the most widely used models for describing drying kinetics of various materials, has demonstrated a strong capability to represent nonlinear moisture reduction behavior and has shown satisfactory performance in previous studies [11]. In this study, model fitting was performed using MATLAB software (Version 2018b). The goodness of fit of the two models was evaluated using the coefficient of determination (R^2) (Eq. (4)) and the root mean square error (RMSE) (Eq. (5)).

$$R^2 = \frac{\sum_{i=1}^{N}\left(MR_{pre,i} - MR_{exp,avg}\right)}{\sum_{i=1}^{N}\left(MR_{exp,i} - MR_{exp,avg}\right)} \tag{4}$$

The coefficient of determination indicates the degree of agreement between the model-predicted values (MR_{pre}) and the experimental data (MR_{exp}), with values closer to unity representing a more satisfactory fit. The root mean square error (RMSE) quantifies the average deviation of model predictions from experimental observations, with lower values indicating higher predictive accuracy, and is defined as:

$$RMSE = \sqrt{\frac{\left(\sum_{i=1}^{N}\left(MR_{pre,i}\right) - \sum_{i=1}^{N}\left(MR_{exp,i}\right)\right)^2}{N}} \tag{5}$$

In Eqs. (3) and (4), $MR_{exp,avg}$ is the average experimental moisture ratio, and (N) is the total number of experimental treatments.

3. Results and discussion

3.1. Chemical characterization of the effluent-derived precipitate

The elemental and chemical composition of the effluent-derived precipitate was analyzed using Inductively Coupled Plasma–Optical Emission Spectroscopy (ICP–OES). The chemical analysis revealed a notably high MgO content (42%), corresponding to the magnesium equivalent in the precipitate, which confirms the substantial presence of magnesium hydroxide in the desalination effluent. In particular, the reduced levels of Na_2O and SO_3 indicate the effective removal of residual sodium salts and sulfate ions from the effluent or reaction medium. This observation is fully consistent with previous studies on magnesium hydroxide recovery from saline and industrial waste streams [12, 13].

The measured loss on ignition (LOI) of 31% suggests the presence of relatively large amounts of adsorbed water and/or hydrated or carbonated species within the precipitate, which are expected to be significantly affected by the drying process. Other detected components were present only in trace amounts. Achieving a constant mass after drying confirmed that the process had reached completion and that further evaporation of moisture or volatile species was negligible [14]. The dried precipitate exhibited favorable physical characteristics, including a uniform white color, a soft powdery texture, and the absence of coarse particles, indicating high purity of the recovered magnesium hydroxide and effective removal of soluble impurities.

3.2. Effect of temperature and pressure on drying time

Magnesium hydroxide samples were dried in the vacuum dryer at three temperature levels (150, 210, and 250°C) and three absolute pressure levels (0.10, 0.05, and 0.02bar). Total drying time was selected as the primary performance indicator, and the corresponding results are summarized in Table 1. As observed, both temperature and pressure exerted statistically significant effects on the drying time.

At a constant pressure of 0.10bar, increasing the temperature from 150 to 250°C reduced the average drying time from 73 to 44.5min, corresponding to an approximate 39% reduction in process duration. A similar trend was observed at lower pressure levels. At 0.05 bar, the drying time decreased from 53 min at 150°C to 30.5 min at 250°C, representing a reduction of approximately 42%.

Conversely, at a fixed temperature of 150°C, reducing the pressure from 0.10 to 0.02 bar shortened the drying time from 73 to 35.5min, corresponding to an approximate 51% reduction. This pressure-dependent behavior was consistently observed at 210 and 250°C. The minimum drying time (22.5min) was achieved at 250°C and 0.02bar, which represents an overall reduction of approximately 69% compared with the baseline condition of 150°C and 0.10bar.

These results clearly demonstrate that decreasing the operating pressure enhances the vapor pressure gradient and accelerates mass transfer, while increasing temperature raises the available thermal energy and promotes moisture evaporation. The simultaneous application of low pressure and elevated temperature therefore produces a synergistic effect, leading to a substantial reduction in overall drying time.

Table 1. Measured drying times under varying operational temperatures and pressures

Temperature (°C)	Pressure (bar)	Drying time (min) Treatment 1	Drying time (min) Treatment 2	Average drying time (min)
150	0.10	72	74	73
	0.05	54	52	53
	0.02	36	35	35.5
210	0.10	57	58	57.5
	0.05	40	42	41
	0.02	28	27	27.5
250	0.10	44	45	44.5
	0.05	31	30	30.5
	0.02	22	23	22.5

To evaluate the effects of operational parameters on drying time, the experimental data were statistically analyzed using analysis of variance (ANOVA). In this analysis, temperature and pressure were considered as independent variables, while drying time was treated as the dependent variable. The ANOVA results, including the main effects of temperature and pressure on drying time, are presented in Table 2. The analysis revealed that the corrected statistical model exhibited a high explanatory power and was overall statistically significant (Sig<0.001), indicating that the selected independent variables account for a substantial proportion of the variability in drying time.

Examination of the main effects demonstrated that temperature had a statistically significant influence on the drying time of magnesium hydroxide samples (F=685.389, Sig<0.001), such that variations in temperature resulted in pronounced changes in process duration. Similarly, operating pressure, as an independent factor, showed a highly significant effect on drying time (F=1342.389, Sig<0.001), highlighting the strong sensitivity of the vacuum drying process to pressure variations.

Table 2. ANOVA results for the effect of temperature and pressure on drying time

Source	Type III Sum of squares	df	Mean Square	F	Sig.
Corrected Model	4178.111[a]	8	522.264	522.264	.000
Intercept	32938.889	1	32938.889	32938.889	.000
Temperature	1370.778	2	685.389	685.389	.000
Pressure	2684.778	2	1342.389	1342.389	.000
Temperature*Pressure	122.556	4	30.639	30.639	.000
Error	9.000	9	1.000		
Total	37126.000	18			
Corrected Total	4187.111	17			

In addition to the main effects, the interaction between temperature and pressure was also found to be statistically significant (F=30.639, Sig<0.001). This result indicates that the effects of temperature and pressure are not independent; rather, simultaneous changes in these parameters can markedly alter the drying behavior (Fig. 4). In other words, the influence of temperature on drying time depends on the applied pressure level, and vice versa.

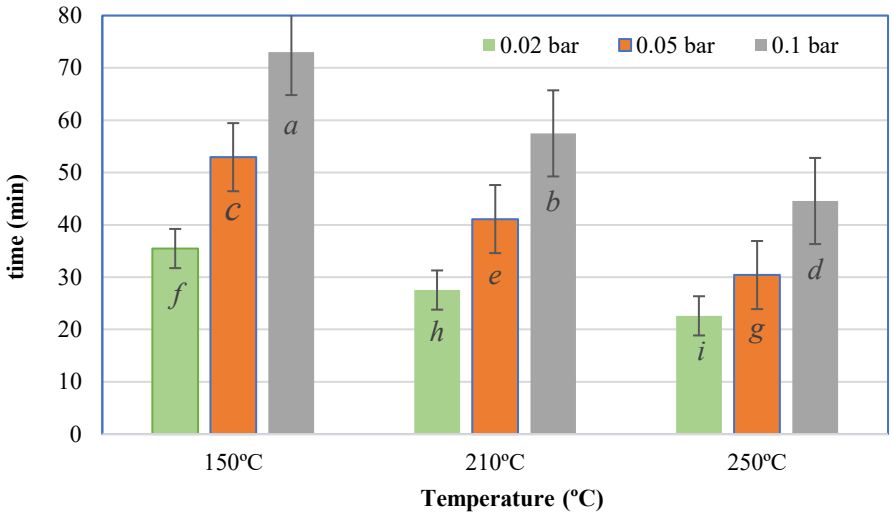

Fig. 4. Interaction effect of temperature and pressure on drying time of magnesium hydroxide. Different letters in the figure indicate statistically significant differences among treatments

A substantial reduction in drying time was observed as pressure decreased from 0.10 to 0.02bar (Fig. 5). For instance, at 150°C, the drying time decreased from 72min (0.10bar) to 36min (0.02bar). At 210°C, the corresponding reduction was from 57 to 28min, while at 250°C, drying time decreased from 44 to 22 min. This pronounced reduction can be attributed to two primary mechanisms: (I) the decrease in the equilibrium vapor pressure of water and the associated reduction in boiling temperature [15], and (II) the increase in the pressure gradient between the vapor released from the sample surface and the drying chamber, which accelerates evaporation. For example, at a wall temperature of 150°C, reducing the pressure from 0.10 to 0.02bar resulted in a decrease in drying time from 72 to 36min, corresponding to a 50% reduction in process duration solely due to pressure reduction.

The findings of this study demonstrate that temperature and pressure exert a synergistic effect during vacuum drying of magnesium hydroxide samples. Specifically, reducing pressure to 0.02 bar while simultaneously increasing wall temperature from 150 to 250°C led to an effective reduction in drying time from 36 to 22 min. This condition corresponded to the shortest drying time observed across all experimental runs. The underlying mechanism can be attributed to the combined enhancement of internal heat transfer and the increased rate of water evaporation under very low-pressure conditions.

Previous studies have reported similar synergistic behavior in the vacuum drying of mineral materials, particularly magnesium hydroxide. Accordingly, simultaneous control of pressure and temperature is essential for achieving rapid and economically efficient drying. One of the major advantages of vacuum dryers lies in their ability to precisely regulate these parameters and adapt them to product requirements and thermodynamic constraints [5].

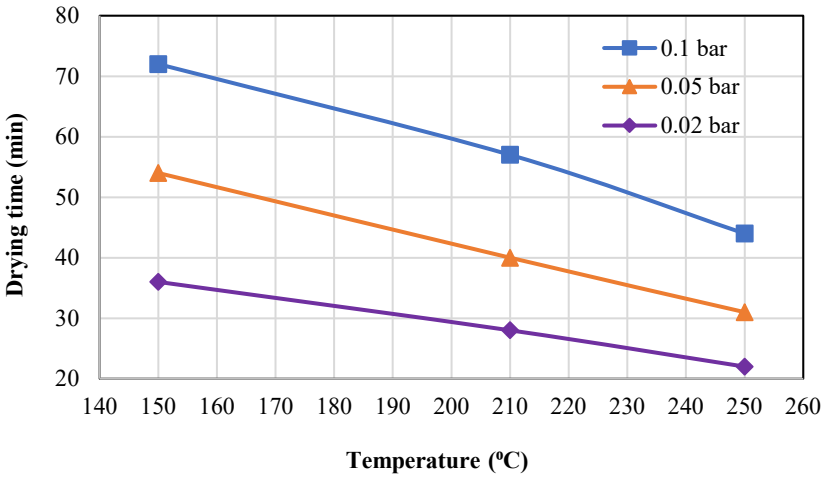

Fig. 5. Drying time versus dryer body temperature at different pressures

Earlier investigations have shown that selecting moderate drying temperatures (approximately 60–75°C) for hydroxyl-containing materials such as magnesium hydroxide yields optimal performance in terms of preserving crystalline order and preventing premature dehydration [16]. In the present study, following completion of the drying process, the sample mass remained constant over successive measurements, confirming attainment of constant weight and completion of drying [5]. The dried samples exhibited a uniform white color, a soft texture, and the absence of coarse particles, indicating high purity and effective removal of soluble impurities during the washing stage. These characteristics are consistent with previously reported properties of vacuum-dried $Mg(OH)_2$ powders [17]. Overall, the results confirm that vacuum drying at moderate temperatures is an efficient method for moisture removal without damaging the crystalline structure of $Mg(OH)_2$, leading to the production of a soft, white, and homogeneous powder with favorable surface properties [16-18].

3.3. Drying kinetics

The moisture ratio (MR) versus time curves obtained for the nine experimental treatments, comprising three temperature levels and three pressure levels, clearly illustrate the kinetic behavior of the drying process (Fig. 6). In general, for all treatments, the reduction in moisture ratio with time followed a nonlinear trend, which is a characteristic feature of most drying processes involving solid and semi-solid materials.

During the initial stages of drying, the curves exhibited relatively steep slopes, indicating a rapid decrease in moisture ratio. This behavior corresponds to the removal of free and surface moisture from the samples. As drying progressed, the slope of the curves gradually decreased, and the process entered the falling-rate period, during which moisture transport is predominantly governed by internal diffusion mechanisms. The absence of a distinct constant-rate drying period in most treatments suggests that moisture diffusion within the material structure is the dominant controlling mechanism throughout the drying process.

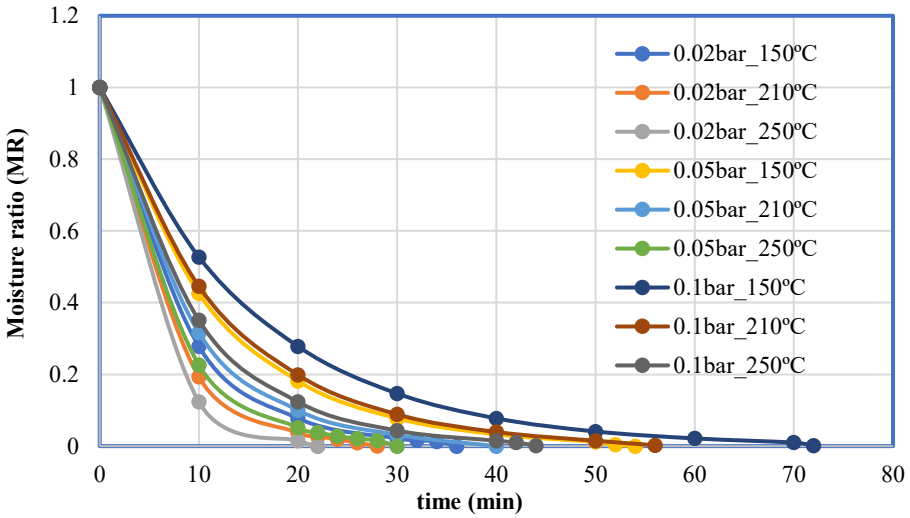

Fig. 6. Drying curves of magnesium hydroxide under varying temperatures and pressures

An increase in temperature at all pressure levels accelerated moisture removal and reduced the overall drying time by enhancing effective moisture diffusivity and mass transfer rates, making temperature a key governing parameter in drying kinetics. In addition, pressure reduction significantly improved drying performance by increasing the driving force for mass transfer, resulting in lower moisture ratios at a given time. Overall, the results confirm a strong coupled thermo-pressure effect in the vacuum drying process.

3.4. Drying kinetics modeling

The results of kinetic modeling using the logarithmic and two-term exponential models demonstrated that both models are capable of adequately describing the evolution of moisture ratio under different temperature and pressure conditions, as evidenced by the high values of the coefficient of determination (R^2) obtained for all treatments. However, comparison of the statistical goodness-of-fit indicators revealed that the logarithmic model provided a more accurate representation of the experimental data, as indicated by its lower RMSE values.

This finding suggests that the logarithmic model has a superior ability to capture the nonlinear behavior of moisture transport during vacuum drying of magnesium hydroxide. In contrast, the two-term exponential model exhibited higher sensitivity to changes in operating conditions (temperature and pressure), which led to increased prediction errors in certain treatments. These results imply that, despite its greater structural complexity, the multi-exponential model does not necessarily improve predictive accuracy under all conditions.

The obtained modeling performance (logarithmic model: R^2=0.992–0.998, RMSE=0.003–0.009; two-term exponential model: R^2=0.985–0.993, RMSE=0.010–0.021) is consistent with values reported by Doymaz [19], where drying models for carrot slices yielded R^2 values in the range of 0.990–0.997. Similarly, Mortezapour et al. [20] reported logarithmic-type models with $R^2 \approx 0.988$–0.996 in solar drying systems, and Rostami et al. [21] observed effective diffusivity-based fits with R^2 around 0.984–0.995 under microwave drying conditions. Moreover, the magnitude of model performance indicators in the present study falls within the same statistical range as these published works, confirming the reliability of the fitted kinetic parameters and supporting the applicability of the logarithmic model for vacuum drying of magnesium hydroxide.

Although the logarithmic model showed the best statistical fit (R^2 = 0.99, RMSE = 0.012), it also has clear physical significance. Its suitability indicates that drying occurs predominantly in the falling rate period, governed by internal

moisture diffusion. Under vacuum conditions, rapid evaporation of free surface moisture leads to an initial sharp decline in moisture ratio, followed by a gradual decrease as internal mass transfer resistance increase. The logarithmic model effectively captures this transition from surface evaporation to diffusion-controlled drying, unlike simpler exponential models. This suggests that internal diffusion resistance dominates most of the process, particularly at later stages. Consequently, while reduced pressure accelerates early drying, its influence diminishes once the diffusion-controlled regime is reached.

Accordingly, the selection of the logarithmic model for predicting the drying behavior of magnesium hydroxide in a vacuum dryer can be considered both statistically and practically justified. The corresponding modeling results are summarized in Table 3.

Table 3. Model fitting analysis for logarithmic and two-term exponential models at different operational conditions

Model	Pressure (bar)	Temp. (°C)	R^2	RMSE
Logarithmic	0.02	150	0.99990818	0.00428961
		210	0.99992475	0.00388788
		250	0.99993337	0.00678734
	0.05	150	0.99992369	0.00359315
		210	0.99993472	0.00475163
		250	0.99987635	0.00449925
	0.1	150	0.99994622	0.00283013
		210	0.99995909	0.00284245
		250	0.9999464	0.00327398
Two-term exponential	0.02	150	0.99987679	0.00444444
		210	0.99986513	0.00465568
		250	0.99985948	0.00696959
	0.05	150	0.9998091	0.00518791
		210	0.99985718	0.00573864
		250	0.99983811	0.00469962
	0.1	150	0.99991814	0.00323268
		210	0.99990889	0.0037941
		250	0.99990719	0.00385333

The estimated parameters and model constants of the logarithmic model for fitting the drying kinetics of magnesium hydroxide at different temperature and pressure levels are presented in Table 4. Owing to its semi-empirical structure, this model exhibits a strong capability to describe the nonlinear decrease in moisture ratio during drying and has therefore been widely employed in kinetic studies.

Table 4. Logarithmic model fitting parameters for predicting magnesium hydroxide drying behavior

Model	Pressure (bar)	Temperature (°C)	a	k	c
Logarithmic	0.02	150	1.003	0.1268	-0.0031
		210	1.004	0.1619	-0.00454
		250	1.007	0.2044	-0.00663
	0.05	150	1.005	0.08396	-0.00592
		210	1.006	0.1132	-0.00639
		250	1.003	0.1466	-0.0036
	0.1	150	1.003	0.06344	-0.00305
		210	1.004	0.07985	-0.00451
		250	1.003	0.1037	-0.00355

Coefficients (with 95% confidence bounds) $MR = a.exp(-kt) + c$

3.5. Model validation and predictive performance

The comparison plots between experimental and predicted moisture ratio values further confirm the suitability of the logarithmic model as the optimal kinetic model (Fig. 7). The excellent agreement between measured data and model predictions under all operating conditions demonstrates the high accuracy of the logarithmic model in representing the actual drying behavior.

The substantial overlap between experimental data points and predicted curves, particularly over the entire drying period from the initial stage to low moisture contents, indicates that the logarithmic model is capable of describing nonlinear moisture ratio variations with satisfactory precision. Such close agreement between experimental observations and predicted results validates the logarithmic model both statistically and visually.

Overall, these findings demonstrate that the logarithmic model can be reliably employed as an effective tool for analyzing and predicting the vacuum drying behavior of magnesium hydroxide. The results are also aligned with previous studies emphasizing the effectiveness of simple and interpretable models in describing the drying kinetics of mineral and industrial materials, thereby providing strong scientific justification for the selection of the logarithmic model in the present work.

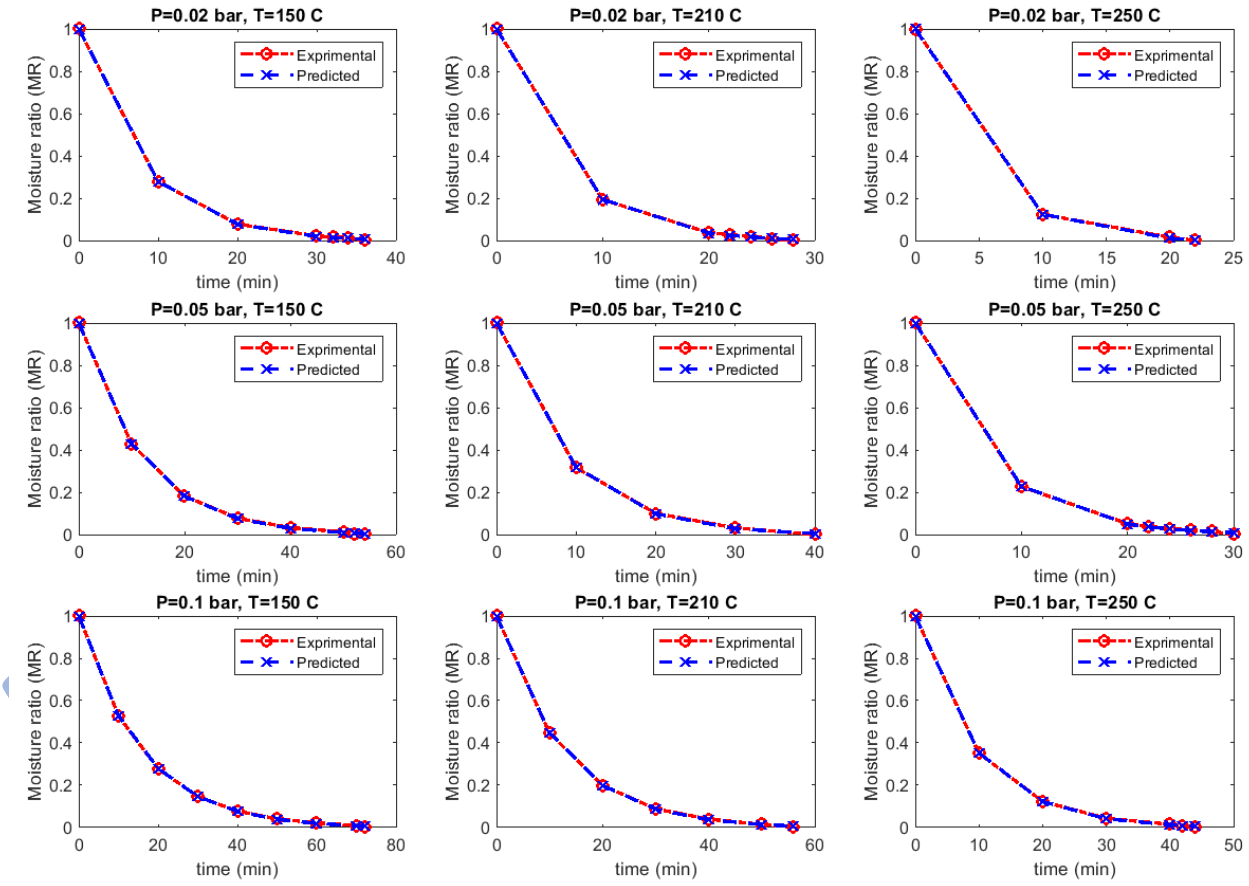

Fig. 7. Comparison of experimental and logarithmic model–predicted drying behavior of magnesium hydroxide at different operational conditions

4. Conclusion

This study demonstrated efficient magnesium recovery from desalination effluent via vacuum drying of precipitated magnesium hydroxide, achieving over 95% recovery efficiency. Drying performance was strongly influenced by temperature and pressure: higher temperatures improved heat transfer, while lower pressures enhanced mass transfer

by reducing the water boiling point. The shortest drying time (22min) occurred at 250°C and 0.02bar, whereas the longest (72min) was at 150°C and 0.10bar. High-temperature/low-pressure conditions consistently accelerated moisture removal compared to low-temperature/high-pressure conditions. Moisture ratio–time curves indicated drying occurred predominantly in the falling-rate period, confirming diffusion-controlled moisture transport. Statistical analysis verified significant synergistic effects of temperature and pressure on drying kinetics, highlighting the need for simultaneous optimization. Kinetic modeling showed the logarithmic model outperformed the two-term exponential model across all conditions, yielding the highest coefficients of determination (R^2=0.99) and demonstrating superior predictive accuracy. Strong agreement between experimental and predicted moisture ratios validated the model's reliability. Overall, vacuum drying with optimized thermal and pressure conditions, combined with industrial waste heat utilization, offers an efficient, robust, and industrially viable approach for sustainable magnesium hydroxide recovery from desalination effluents.

Acknowledgement

The authors gratefully acknowledge Hormozgan Aluminum Facilities for their valuable contributions and for providing the laboratory equipment.

Nomenclature

Symbols		Abbreviation	
T	Temperature (°C)	ICP–OES	Inductively Coupled Plasma–Optical Emission Spectroscopy
t	Time (s)	RCBD	Randomized Complete Block Design
W	Power (Watt)	ANOVA	Analysis of Variance
pH	Acidity/basicity	RMSE	Root Mean Square Error
a, c	Logarithmic model constants	MR	Moisture Ratio
a_0, a_1	Coefficients in two–term exponential model	MR_pre	Predicted Moisture Ratio
k	Drying constant in logarithmic model	MR_exp	Experimental Moisture Ratio
k_0, k_1	Drying constants in two–term exponential model	LOI	Loss on Ignition (%)
R^2	Coefficient of determination		
N	Total number of experimental data		

References

[1] Polmear, I., StJohn, D., Nie, J.-F., Qian, M., 2017. Light alloys: metallurgy of the light metals. https://doi.org/10.1016/B978-0-08-099431-4.00001-4
[2] Fontana, D., Forte, F., Pietrantonio, M., Pucciarmati, S., Marcoaldi, C., 2023. Magnesium recovery from seawater desalination brines: a technical review, Environment, Development and Sustainability, 25(12), 13733–13754. https://doi.org/10.1007/s10668-022-02663-2
[3] Pan, S.-Y., Chiang, P.-C., Chen, Y.-H., Tan, C.-S., Chang, E., 2013. Ex situ CO_2 capture by carbonation of steelmaking slag coupled with metalworking wastewater in a rotating packed bed, Environmental Science and Technology, 47(7), 3308–3315. https://doi.org/10.1021/es304975y
[4] Li, P., Ma, C., Chen, Z., Wang, H., Wang, Y., Bai, H., 2023. A review: study on the enhancement mechanism of heat and moisture transfer in deformable porous media, Processes, 11(9), 2699. https://doi.org/10.3390/pr11092699
[5] Mujumdar, A.S., 2014. The making of the handbook of industrial drying, Vol. 32, Taylor and Francis, 627–628.
[6] Pasten, A., Vega-Galvez, A., Uribe, E., Carvajal, M., Mejías, N., Araya, M., Goñi, M.G., 2024. A comparison of the effects of low-temperature vacuum drying and other methods on cauliflower's nutritional–functional properties, Processes, 12(8), 1629. https://doi.org/10.3390/pr12081629
[7] Mansour, N.E., Metwally, K.A., Tantawy, A.A., Elbeltagi, A., Salem, A., Dewidar, A.Z., Okasha, A.M., Moustapha, M.E., Elwakeel, A.E., 2025. Automated vacuum drying kinetics, thermodynamics, and economic analysis of sage leaves, Scientific Reports, 15(1), 18779. https://doi.org/10.1038/s41598-025-03367-z
[8] Šooš, Ľ., Urban, F., Čačková, I., Kolláth, Ľ., Mlynár, P., Čačko, V., Bábics, J., 2024. Analysis of thermodynamic events taking place during vacuum drying of corn, Sustainability, 16(2), 879. https://doi.org/10.3390/su16020879
[9] Droste, R.L., Gehr, R.L., 2018. Theory and practice of water and wastewater treatment, John Wiley and Sons.

[10] Jouhara, H., Khordehgah, N., Almahmoud, S., Delpech, B., Chauhan, A., Tassou, S.A., 2018. Waste heat recovery technologies and applications, Thermal Science and Engineering Progress, 6, 268–289. https://doi.org/10.1016/j.tsep.2018.04.017
[11] Tehranizade Kermani, N., Maharlooei, M., Mortezapour, H., 2020. Study the drying kinetics, energy consumption and quality parameters of Echium amoenum in an IR equipped solar dryer, Journal of Food Science and Technology (Iran), 17(102), 161–174. https://doi.org/10.52547/fsct.17.102.161 [in Persian].
[12] Battaglia, G., Romano, S., Raponi, A., Marchisio, D., Ciofalo, M., Tamburini, A., Cipollina, A., Micale, G., 2022. Analysis of particle size distributions in $Mg(OH)_2$ precipitation from highly concentrated $MgCl_2$ solutions, Powder Technology, 398, 117106. https://doi.org/10.1016/j.powtec.2021.117106
[13] Tan, K.E.B., Choi, A.E.S., 2023. Development of separation techniques for magnesium recovery: a mini-review, Chemical Engineering Transactions, 106, 55–60. https://doi.org/10.3303/CET23106010
[14] Romano, S., Trespi, S., Achermann, R., Battaglia, G., Raponi, A., Marchisio, D., Mazzotti, M., Micale, G., Cipollina, A., 2023. The role of operating conditions in the precipitation of magnesium hydroxide hexagonal platelets using NaOH solutions, Crystal Growth & Design, 23(9), 6491–6505. https://doi.org/10.1021/acs.cgd.3c00462
[15] Bergman, T.L., 2011. Fundamentals of heat and mass transfer, John Wiley and Sons.
[16] Silva Neto, L.D., Anchieta, C.G., Duarte, J.L., Meili, L., Freire, J.T., 2021. Effect of drying on the fabrication of MgAl layered double hydroxides, ACS Omega, 6(33), 21819–21829. https://doi.org/10.1021/acsomega.1c03581
[17] Piperopoulos, E., Fazio, M., Mastronardo, E., Lanza, M., Milone, C., 2021. Tuning $Mg(OH)_2$ structural, physical, and morphological characteristics for its optimal behavior in a thermochemical heat-storage application, Materials, 14(5), 1091. https://doi.org/10.3390/ma14051091
[18] Luo, S., Liu, M., Yang, L., Chang, J., 2019. Effects of drying techniques on the crystal structure and morphology of ettringite, Construction and Building Materials, 195, 305–311. https://doi.org/10.1016/j.conbuildmat.2018.11.078
[19] Doymaz, İ., 2017. Drying kinetics, rehydration and colour characteristics of convective hot-air drying of carrot slices, Heat and Mass Transfer, 53(1), 25–35. https://doi.org/10.1007/s00231-016-1791-8
[20] Mortezapour, H., Noroozi, A., Abdi, A., 2024. Development of an indirect forced flow greenhouse solar dryer for barberry drying, Biomechanism and Bioenergy Research, 3(2), 31–38. https://doi.org/10.22103/BBR.2024.22906.1079
[21] Rostami, A., Jafarinaeimi, K., Maghsoudi, H., 2025. Mathematical modeling and investigation of the effect of power on effective moisture diffusivity and activation energy of turnip slices in microwave drying, Biomechanism and Bioenergy Research, 4(2), 26–39. https://doi.org/10.22103/BBR.2025.24863.1117